Journal of Solid State Chemistry **142,** 138–145 (1999)
Article ID jssc.1998.8002, available online at http://www.idealibrary.com on IDEAL®

Synthesis of $AFeO_{2.5+x}$ ($0 \leq x \leq 0.5$; A = Sr, Ca) Mixed Oxides from the Oxidative Thermal Decomposition of $A[Fe(CN)_5NO] \cdot 4H_2O$

María Inés Gómez*, Juana A. de Morán*, Raúl E. Carbonio,†,[1,2] and Pedro J. Aymonino‡,[2]

*Instituto de Química Inorgánica, Facultad de Bioquímica, Química y Farmacia. Universidad Nacional de Tucumán, Ayacucho 491, 4000 S. M. de Tucumán, Argentina; †INFIQC, Departamento de Físico Química, Facultad de Ciencias Químicas, Universidad Nacional de Córdoba, Ciudad Universitaria 5000 Córdoba, Argentina; ‡CEQUINOR (CONICET, UNLP) and LANAIS EFO (CONICET, UNLP), Departamento de Química, Facultad de Ciencias, Exactas, Universidad Nacional de La Plata, CC 962, 1900 La Plata, Argentina

Received September 11, 1997; in revised form August 10, 1998; accepted August 11, 1998

The low-temperature formation of Sr and Ca ferrates by thermal oxidative decomposition of tetrahydrates of Sr and Ca nitroprussides (pentacyanonitrosilferrates(II)) is reported. IR spectroscopy, X-ray diffraction (including Rietveld analysis), and thermal analysis were used to follow the process. The amount of active oxygen (concentration of Fe(IV)) in the products was chemically determined. For the Sr compound, the final product was an oxygen-deficient perovskite that could be produced with a very low content of carbonate in the temperature range 750–850°C. For the calcium compound, only $Ca_2Fe_2O_5$ with the brownmillerite type structure was obtained.

INTRODUCTION

The synthesis of mixed oxides, particularly perovskites and related oxides, from the decomposition of inorganic coordination compounds allows one to lower the reaction temperature and to obtain more homogeneous and finely divided powders (1–5).

Iron(IV)-containing perovskites are extensively used in catalysis (6–12) and electrocatalysis (13–19). Their applications are largely related to oxidations and electrooxidations. These properties should be related to the high oxidizing power of Fe(IV), which, for example, has been specifically recognized to play a significant role in the catalytic oxidative dehydrogenation of ethane on titanium-containing perovskites (11). Fe(III)-containing mixed oxides were reported to have good catalytic activity for NO decomposition (20).

In the synthesis of compounds of the system $AFeO_{2.5+x}$ (where A is Ca^{2+}, Sr^{2+}, or Ba^{2+}), if a perovskite-type structure is formed, oxygen vacancies are usually present (21–24) due to the difficulty in generating Fe(IV), and in the extreme case when $x = 0$, a brownmillerite-type oxide is formed ($A_2Fe_2O_5$) with all of the iron in the +3 oxidation state (22, 25, 26). Brownmillerite-type $Ca_2Fe_2O_5$, with interstitial O, has been obtained at high O_2 pressures (27, 28). Stoichiometric $AFeO_3$ is formed only at extremely high oxygen pressures, 89 MPa for 1 week at 628 K for $SrFeO_3$ (24, 29) and 2 GPa at 1273 K for $CaFeO_3$ (24, 30).

$AFeO_{2.5+x}$ is a model system to study catalytic reactions under oxidizing or reducing conditions, because by changing the oxygenation (the x value), one can tailor the relation Fe(IV)/Fe(III) to specific needs.

The generation of oxygen vacancies in the perovskite structure is increased in these systems as the synthesis temperature increases. Temperatures as high as 1400°C are sometimes used to produce well-defined structures. In such cases, oxygenation at lower temperatures is needed to decrease the number of oxygen vacancies (21). In addition, high temperatures favor the sintering of materials. Thus, for catalytic purposes, low temperatures are needed to produce high surface area catalysts with a high content of Fe(IV) (6–15, 17, 18). For these reasons, low-temperature synthetic methods are crucial in these systems.

In the present work we report the low-temperature synthesis of Sr and Ca ferrates by thermal oxidative decomposition of Sr and Ca nitroprussides, which produces high surface area powders at lower temperatures than the conventional syntheses.

EXPERIMENTAL

$Sr[Fe(CN)_5NO] \cdot 4H_2O$ and $Ca[Fe(CN)_5NO] \cdot 4H_2O$ were prepared by double decomposition reaction between silver nitroprusside and the chlorides or sulfates of the alkaline-earth metals, as already described (31).

$AFeO_{2.5+x}$ (A = Sr, Ca) mixed oxides were obtained by the oxidative thermal decomposition of $Sr[Fe(CN)_5NO] \cdot 4H_2O$ and $Ca[Fe(CN)_5NO] \cdot 4H_2O$ in air or pure oxygen as follows. Heat treatment A: samples were introduced into the furnace at room temperature and then heated to the desired

[1] To whom correspondence should be addressed.
[2] Member of the Research Career of the National Scientific and Technological Research Council, Argentina.

0022-4596/99 $30.00

temperature for 12 h and cooled to room temperature. Heat treatment B: samples were introduced into the furnace already heated to the desired temperature, maintained at that temperature for 12 h, and cooled to room temperature. The samples were then thoroughly ground and the same procedure was repeated up to four times.

Infrared spectroscopy (IRS), X-ray diffraction (XRD) (including Rietveld analysis, when possible), and thermogravimetric analysis (TGA) were used to follow the decomposition process. The amount of active oxygen (concentration of Fe(IV)) in the products was determined by dissolving the solid in a HCl concentrated solution with an excess of Fe(II) (Mohr's salt) and subsequent titration of the remaining Fe(II) with potassium dichromate. Results are referred to the quantities of iron present in the decomposed nitroprusside samples.

IR spectra were recorded with FTIR and FTNIR Bruker IFS 66 and Bruker IFS 113v spectrophotometers.

XRD data from powder samples were recorded between 20° and 125° in 2θ in steps of 0.015° using a Philips PW-170 diffractometer with a Cu$K\alpha$ source and a counting time of 10 s per step. Rietveld analysis was performed for some of the X-ray diffractograms using the program DBWS-9411 (32). Several parameters were refined, including background coefficients, zero point, half width Pearson and asymmetry for the peak shape, scale factor, positional, overall thermal, and unit cell parameters.

Scanning electron microscopy (SEM) photographs were taken with a JEOL JSM 35 CF.

TGA was performed with a Shimadzu TGA 50 unit.

Surface areas were determined by the dye adsorption method (33). Methylene blue was used as adsorbate. Even if dye adsorption in solution might have the problem of pore accessibility by the dye molecule, surface areas obtained in the present work (see below) are in the order of areas reported for nonporous materials, in which case the method has been proved to reproduce BET measurements (33).

RESULTS AND DISCUSSION

$SrFeO_{2.5+x}$

In Fig. 1 we show the percentage of residual weight of samples of $Sr[Fe(CN)_5NO]\cdot 4H_2O$ after heat treatment A as a function of temperature. It is clear from the figure that the theoretical weight loss to produce $SrFeO_{2.5+x}$ is reached above ca. 680°C.

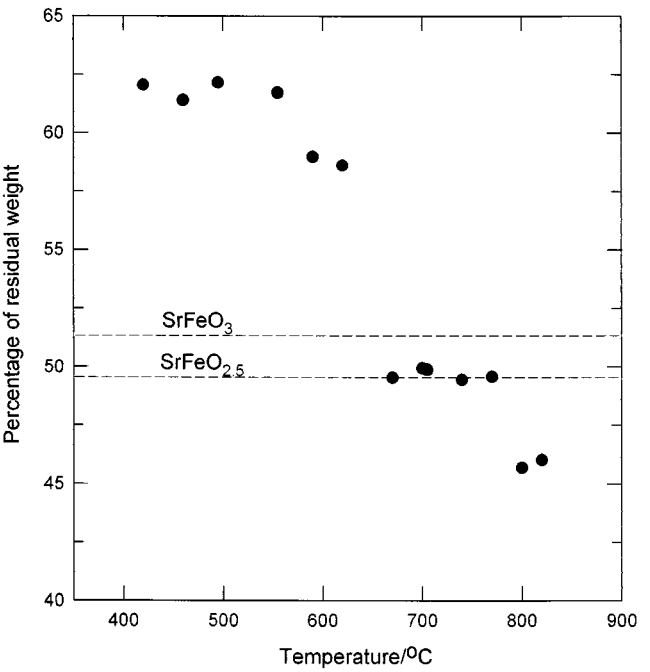

FIG. 1. Percentage of residual weights of samples of $Sr[Fe(CN)_5 NO]\cdot 4H_2O$ after heat treatment A in air at different temperatures. The zone between the dashed lines corresponds to the theoretical weight losses to form $SrFeO_{2.5+x}$ ($0 \le x \le 0.5$).

In Fig. 2 are shown TGA and differential thermogravimetric analytical (DTGA) curves for the decomposition of $Sr[Fe(CN)_5NO]\cdot 4H_2O$ in O_2. They show the loss of water molecules between 25 and 200°C in three steps corresponding to the formation of the dihydrate, the monohydrate, and the anhydrate, respectively (34). In the step centered at ca. 348°C, NO and one CN group ($\frac{1}{2}C_2N_2$) should evolve, as it occurs when heating is made under nitrogen (at 336°C) (34), but in the presence of oxygen a more complicated reaction takes place with further evolution of three additional CN groups and the transformation of the remaining one into carbonate, with formation of the strontium salt. Iron is perhaps oxidized to Fe_2O_3. The corresponding chemical (partial) reaction taking place in this step could be represented as

$$Sr[Fe(CN)_5\ NO] \xrightarrow{O_2} SrCO_3 + Fe_2O_3 + \text{etc.}$$

The weight change expected from this reaction should be practically the same as the change in the (total) dehydration step, as observed in the thermogram of Fig. 2.

The stoichiometry of the last step (DTGA peak at 737°C) seems to correspond to the loss of CO_2 and formation of $SrFeO_{2.5+x}$ (with $x > 0$, as suggested by chemical analysis (see below)) but even at 800°C the presence of some carbonate is still detected by IRS (see Fig. 3).

To discard the possibility that carbonate could be formed by atmospheric CO_2, we repeated the treatment under pure O_2. Carbonate was also detected, so it can be concluded that the oxidation of CN is the source of carbonate. This reaction seems to take place at $T > 400$°C. The CO_2 generated *in situ* should therefore be responsible for the $SrCO_3$ production.

To avoid the formation of carbonate, we developed heat treatment B. Figure 4 shows IR spectra of samples produced

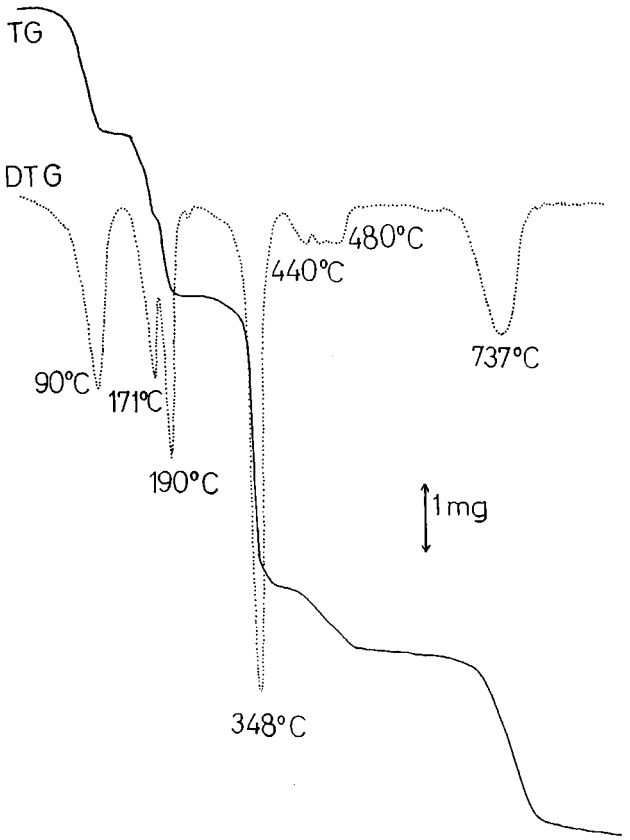

FIG. 2. TGA and DTGA of $Sr[Fe(CN)_5NO]\cdot 4H_2O$ in oxygen. Initial weight: 24 mg.

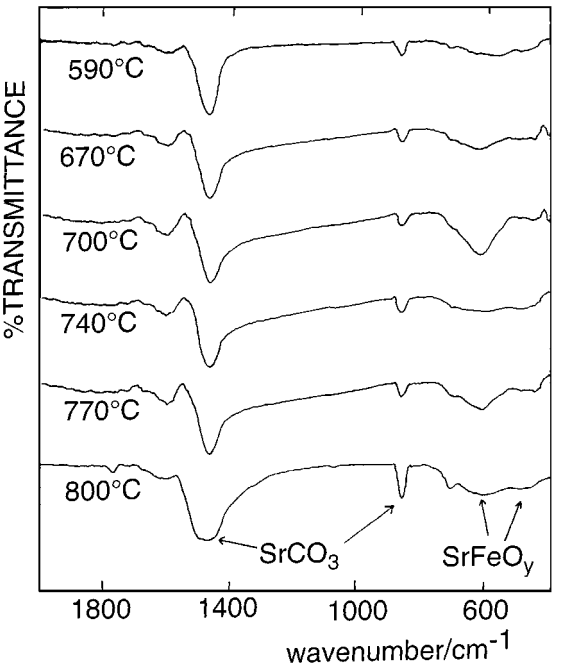

FIG. 3. IR spectra of $Sr[Fe(CN)_5NO]\cdot 4H_2O$ heat treated in air according to method A at different temperatures.

according to this treatment at 830°C with the procedure repeated from one to three times. It is clear that, after three heat treatments at this temperature, carbonate is not detected by IRS. In Fig. 5 we show the IR spectra of two samples prepared according to heat treatment B repeated four times, but at lower temperatures (700 and 750°C), close to the temperature range where the weight loss corresponds to a final product of formula $SrFeO_{2.5+x}$ (Fig. 1).

Clearly, this treatment at 750°C produces a sample with a very low level of carbonate (barely detectable by XRD but not by IRS) and with the $SrFeO_{2.5+x}$ stoichiometry. The x values, determined by chemical analysis, are presented in Fig. 6 for heat treatment B as a function of temperature. Even if IRS and XRD indicate that carbonate is present in the samples at temperatures higher than 700°C (see below), the weight losses (Figs. 1 and 9) indicate that, within the experimental error of the weighing process, at temperatures higher than ca. 650°C, most of the volatile species (coming from the decomposition of CN and NO groups) were already eliminated. Thus assuming that only the mixed oxide and eventually some form of Fe_2O_3 are present in the samples, the meaning of x in Fig. 6 is to give the relative amount of oxygen to the total amount of Fe present in the samples, assuming that their stoichiometric composition is $AFeO_{2.5+x}$.

At $T \leq 600$°C (not shown) $x = 0$. At higher temperatures there is an increase in x, reaching its maximum value at 800°C and then decreasing to very low values close to 850°C. The increase in x as T increases indicates a larger

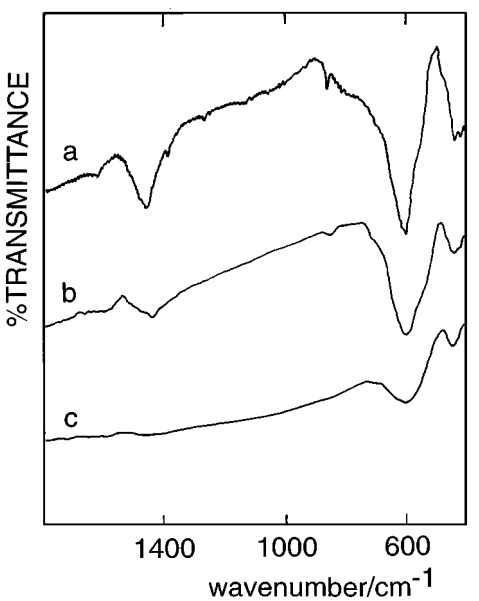

FIG. 4. IR spectra of $Sr[Fe(CN)_5NO]\cdot 4H_2O$ heat treated in air according to method B at 830°C: (a) once; (b) twice; (c) three times.

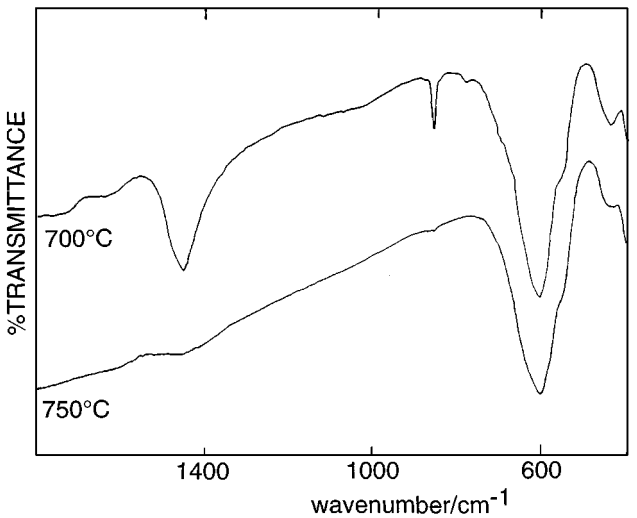

FIG. 5. IR spectra of $Sr[Fe(CN)_5NO]\cdot 4H_2O$ after heat treatment B (four times, 12 h) at two different temperatures.

ability of oxygen to oxidize Fe(III) to Fe(IV) and of the system to build the crystal structure of the mixed oxide ($SrFeO_{2.5+x}$). The further decrease in x has to be assigned to the loss of oxygen from the mixed oxide structure, due to the instability of Fe(IV) at these temperatures. Thus, to get the lowest content of carbonate and the highest of Fe(IV) (oxygen content), the temperature range between 750 and 850°C seems to be optimum.

A complete identification of the synthesized compounds should include a crystallographic characterization. Takeda

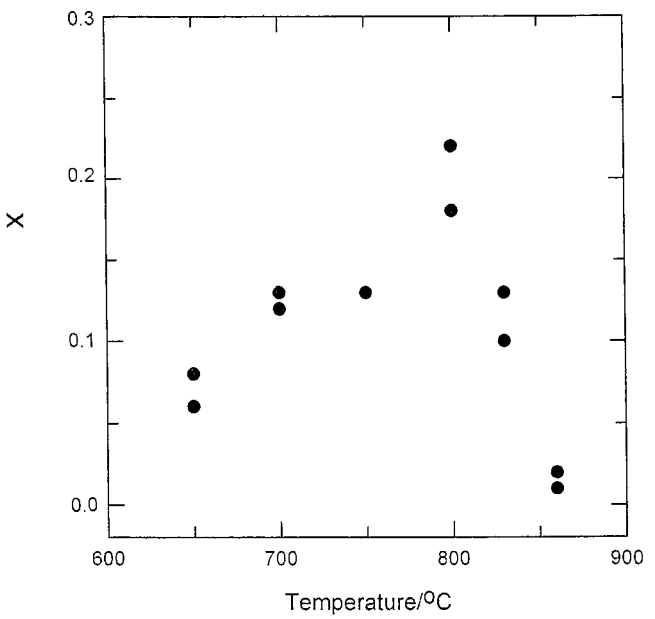

FIG. 6. Oxygen content (x) in $SrFeO_{2.5+x}$ vs temperature of synthesis. Samples were treated in air (heat treatment B) (four times, 12 h).

et al. (21) reported that the $SrFeO_y$ system presented different structures depending on the y value ($y = 2.5 + x$ in our case). Thus, for $2.5 \leq y \leq 2.68$ a brownmillerite-type phase ($Sr_2Fe_2O_5$) and an orthorhombic oxygen-deficient perovskite phase coexist; for $2.68 \leq y \leq 2.74$ there is only the orthorhombic phase. For higher y values, successive regions of coexistence of orthorhombic and tetragonal phases, pure tetragonal phase, tetragonal and cubic phases, and pure cubic phase are observed (21). To identify the phases present in our samples, X-ray diffractograms of samples prepared according to method B repeated four times at 750 and 850°C were obtained. For the sample prepared at 750°C (Fig. 7a), we could not make a clear indexing of the reflections due to their poor definition but we could detect very small amounts of $SrCO_3$ (labeled i) and another impurity which, in principle, could be γ-Fe_2O_3 (maghemite) (labeled x) (35). For the sample prepared at 850°C (Fig. 7b), the amount of impurities decreased very close to the noise level and the reflections were well defined so that the indexing of the diffractogram could be performed. Using the program PIRUM (36) for indexing of reflections and refinement of unit cell parameters, we obtained an orthorhombic cell with $a = 10.9758(6)$, $b = 7.7106(5)$, and $c = 5.4718(3)$ Å. These are very close to those of the orthorhombic cell reported by Takeda *et al.* for $SrFeO_{2.73}$ (21).

SEM photographs of $Sr[Fe(CN)_5NO]\cdot 4H_2O$ calcined at 750°C using heat treatment B (Fig. 8) showed that the average particle size was on the order of 1 μm. Surface areas determined by adsorption with methylene blue are shown in Tables 1 and 2 for products obtained by both methods at different temperatures. Higher surface areas are obtained with method B at the same temperatures. These results may be explained by the fact that with method B during the fast initial heating, violent gas evolution might produce smaller particles and higher surface areas.

Thus, $SrFeO_{2.5+x}$ with a relatively high Fe(IV) content and almost free of carbonate can be produced in the temperature range 750–850°C. These temperatures are sufficiently low to produce a relatively high surface area material that could have good catalytic properties. If higher Fe(IV) contents were desired, oxygenation of the sample in pure oxygen at high pressures and low temperatures ($T < 600$°C) should be performed (21). Because of the relatively low temperatures used for oxygenation, this process will not affect the surface area of the samples and consequently will not deteriorate the performance of the catalyst.

$CaFeO_{2.5.+x}$

In Fig. 9 we show the percentage of residual weight of samples of $Ca[Fe(CN)_5NO]\cdot 4H_2O$ after heat treatment A as a function of temperature. It is clear from the figure that the theoretical weight loss to produce $CaFeO_{2.5}$ is reached after ca. 650°C. In Fig. 10 are shown TGA and DTGA

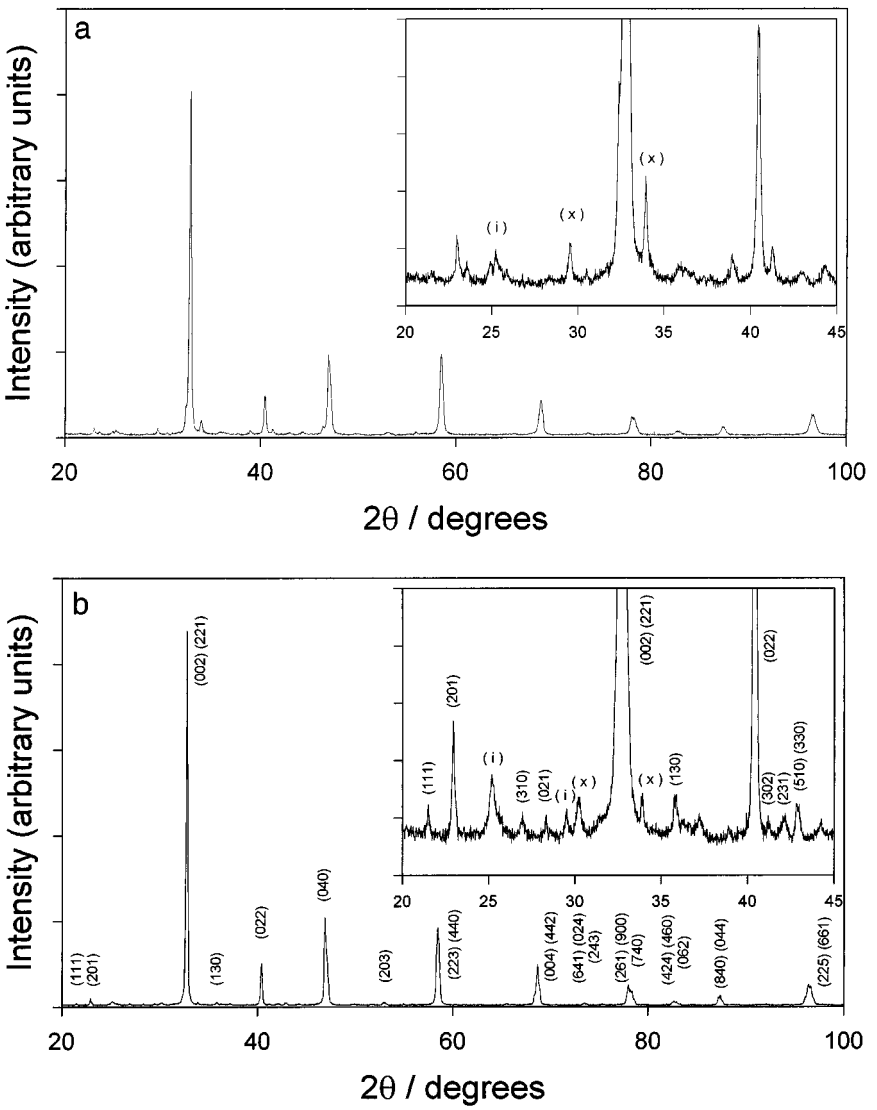

FIG. 7. X-ray diffractograms of samples of $Sr[Fe(CN)_5NO]\cdot 4H_2O$ treated according to method B (four times) at (a) 750 and (b) 850°C. Miller indices of reflections corresponding to $SrFeO_{2.5+x}$ are indicated in the figure. Reflections due to impurities are indicated as (x) for γ-Fe_2O_3 and (i) for $SrCO_3$. The insets show expansions of the 2θ region where the impurities appear.

results for the decomposition of $Ca[Fe(CN)_5NO]\cdot 4H_2O$ in O_2. It shows an initial loss of three water molecules at 72°C. In the step centered at ca. 240°C, the last water molecule is lost. The total weight change of the next three steps up to 800°C taken together corresponds fairly closely with the stoichiometry of the reaction of formation of $Ca_2Fe_2O_5$, but the individual TGA steps are difficult to assign to definite chemical reactions. It is possible that the

TABLE 1
Surface Areas of Residues Obtained by Heat Treatment A of $Sr[Fe(CN)_5NO]\cdot 4H_2O$ at Different Temperatures

Temperature (°C)	Surface area ($m^2\cdot g^{-1}$)
700	1.95
800	1.94
850	1.91
900	1.81

TABLE 2
Surface Areas of Residues Obtained by Heat Treatment B of $Sr[Fe(CN)_5NO]\cdot 4H_2O$ at Different Temperatures

Temperature	Surface area ($m^2\cdot g^{-1}$)
700	3.05
750	2.93
800	2.90
850	2.57
900	2.03

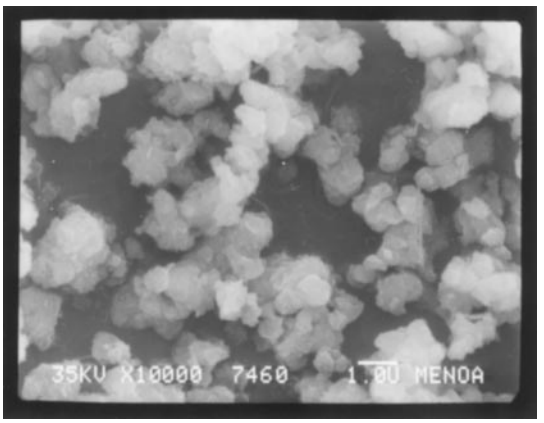

FIG. 8. Scanning electron microscopy of $Sr[Fe(CN)_5NO]\cdot 4H_2O$ heat treated at 750°C (method B, four times).

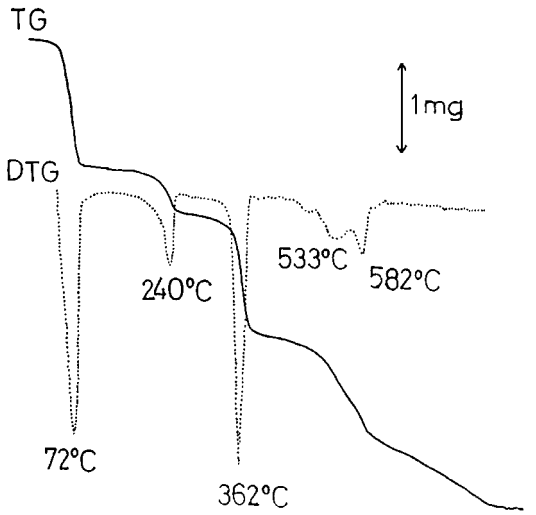

FIG. 10. TGA and DTGA of $Ca[Fe(CN)_5NO]\cdot 4H_2O$ in oxygen. Initial weight: 8.52 mg.

reaction takes a similar course as in the case of $Sr[Fe(CN)_5NO]\cdot 4H_2O$. We do not have enough information to make similar assumptions about the intermediate reactions taking place when the anion is decomposed and its metals transformed in the mixed oxide $Ca_2Fe_2O_5$. In Fig. 11 we show the IR spectra of some of the samples included in Fig. 9. Clearly, even at the higher temperature, $CaCO_3$ is still present. In this case, there is a clear indication in the IR spectra of the temperature at which the mixed oxide starts to develop. The two broad bands in the range 600–900 cm^{-1} correspond to internal modes of the BO_6 octahedra (O_h sites) and BO_4 tetrahedra (T_d sites) in the brownmillerite-type structure (37–39). It is clear that at $T \geq$ 780°C a large amount of the mixed oxide has already been formed. It should be noted that the bands corresponding

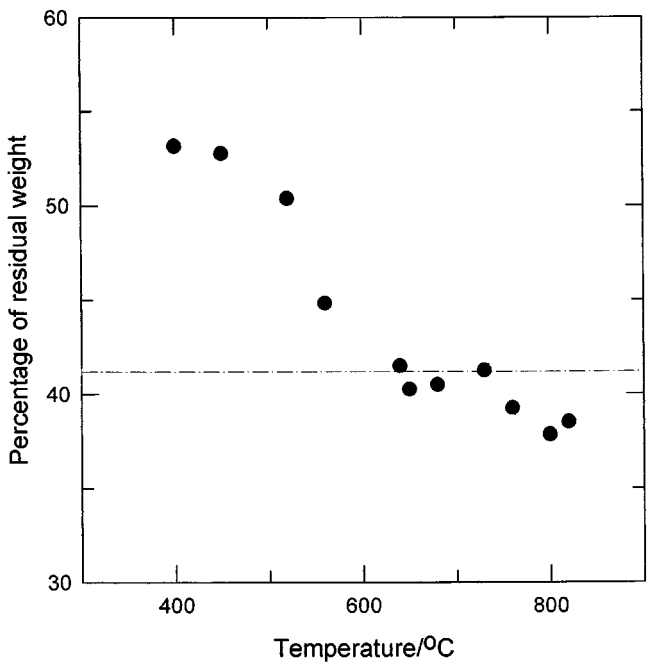

FIG. 9. Percentage of residual weights of samples of $Ca[Fe(CN)_5NO]\cdot 4H_2O$ after heat treatment A in air at different temperatures. The dashed line corresponds to the theoretical weight loss to form $Ca_2Fe_2O_5$.

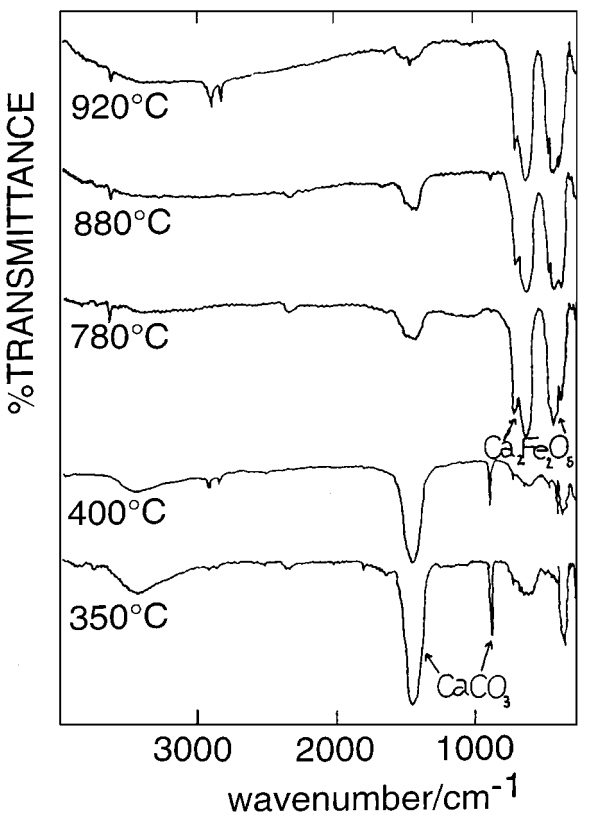

FIG. 11. IR spectra of $Ca[Fe(CN)_5NO]\cdot 4H_2O$ heat treated in air according to method A at different temperatures.

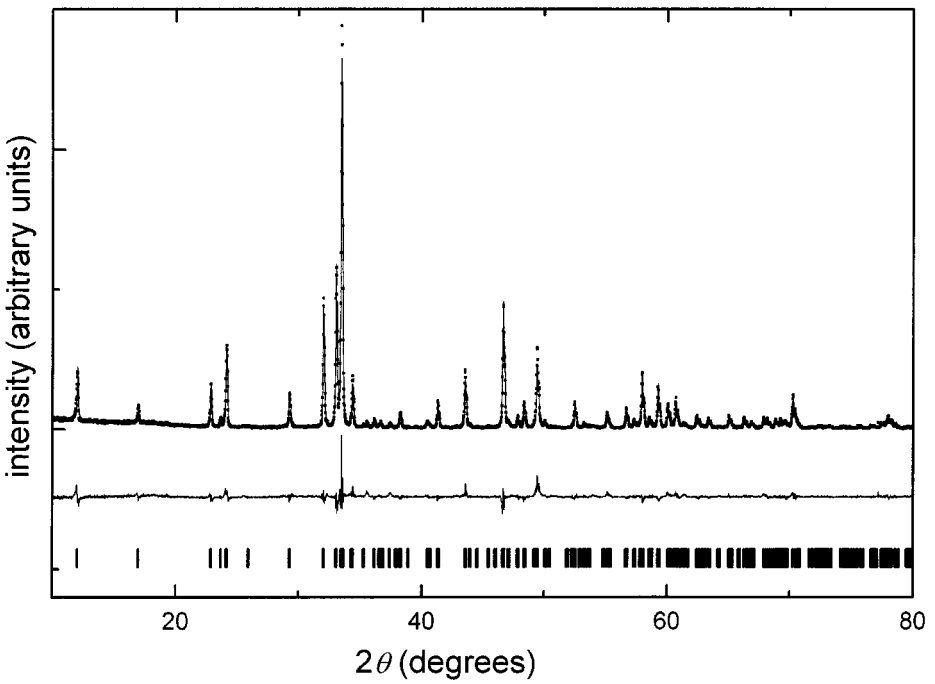

FIG. 12. Rietveld analysis of powder X-ray diffraction data for a sample obtained by heat treatment B (four times) of $Ca[Fe(CN)_5NO]\cdot 4H_2O$ at 850°C in air.

to the O_h sites in the perovskite structure (37) were not clearly developed in the $SrFeO_{2.5+x}$ spectra (Fig. 3). This can be explained by the fact that these bands decrease in relative intensity and eventually disappear when the compound is a metallic conductor (40, 41). These results are in agreement with the fact that $SrFeO_3$ is a metallic conductor (24, 42, 43).

Chemical analyses indicated that, within the experimental error, $x = 0$ for all of the samples, indicating total absence of Fe(IV). The total absence of Fe(IV) in these samples seems reasonable if we consider that a much higher oxygen pressure is needed to synthesize stoichiometric $CaFeO_3$ than $SrFeO_3$ (24, 29, 30), which indicates a much lower stability of Fe(IV) in the $CaFeO_{2.5+x}$ structure than in the $SrFeO_{2.5+x}$ one.

The X-ray diffractogram of a sample prepared according to method B at 850°C (Fig. 12) could be refined by Rietveld analysis using the structural model of brownmillerite-type $Ca_2Fe_2O_5$ (25). The refined cell parameters were $a = 5.4262$, $b = 14.7618$, and $c = 5.5972$ Å. The obtained R factors were $R_{wp} = 15.85\%$, $R_p = 11.77\%$, and S (goodness of fit) $= 1.88$.

Thus, $Ca_2Fe_2O_5$ with a very low content of carbonate could be produced at $T \geq 850$°C. Although in this case no Fe(IV) was present in the samples synthesized in air, again, oxygenation at low temperatures and high oxygen pressures can be used to increase the Fe(IV) content, without decreasing the surface area.

CONCLUSIONS

In the temperature range between 750 and 850°C, the thermal decomposition of $Sr[Fe(CN)_5NO]\cdot 4H_2O$ produces an oxygen-deficient perovskite ($SrFeO_{2.5+x}$) with very small amounts of $SrCO_3$ and γ-Fe_2O_3. At 750°C the perovskite is crystallographically not very well defined but at 850°C, all of the reflections corresponding to the perovskite phase could be indexed with an orthorhombic cell with parameters $a = 10.9758(6)$, $b = 7.7106(5)$, and $c = 5.4718(3)$ Å. These are very close to those of the orthorhombic cell reported for $SrFeO_{2.73}$. Impurities ($SrCO_3$ and γ-Fe_2O_3) are very low in the residues obtained at 850°C.

At temperatures lower than 780°C, the thermal decomposition of $Ca[Fe(CN)_5NO]\cdot 4H_2O$ produces a mixture of $CaCO_3$ (calcite) and probably amorphous mixed oxides of Ca and Fe. At higher temperatures, we find the formation of $Ca_2Fe_2O_5$ with the brownmillerite-type structure.

ACKNOWLEDGMENTS

R.E.C. thanks the Consejo de Investigaciones Científicas y Tecnológicas de la Provincia de Córdoba, the Secretaría de Ciencia y Técnica of the Universidad Nacional de Córdoba, and the Fundación Antorchas for research grants. M.I.G. and J.A. de M. thank CIUNT for financial support. P.J.A. thanks CONICET and CICPBA for providing financial help to CEQUINOR (CONICET, UNLP). We thank Dr. D. B. Soria (CEQUINOR) for her help with TGA and DTA measurements and

L. M. Castro and L. Reinaudi (INFIQC) for technical assistance with the figures.

REFERENCES

1. S. Nakayama, M. Sakamoto, K. Matsuki, Y. Okimura, R. Ohsumi, Y. Nakayama, and Y. Sadaoka, *Chem. Lett*. 2145 (1992).
2. S. Nakayama and M. Sakamoto, *J. Ceram. Soc. Jpn.* **100,** 354 (1992).
3. A. S. Brar, S. Brar, and S. S. Sandhu, *J. Therm. Anal.* **31,** 1083 (1986).
4. M. Sakamoto, K. Matsuki, R. Ohsumi, Y. Nakayama,Y. Sadaoka, S. Nakayama, N. Matsumoto, and H. Okawa, *J. Ceram. Soc. Jpn.* **100,** 1211 (1992).
5. J. M. D. Tascón, S. Mendioroz, and L. González Tejuca, *Z. Phys. Chem.* (*Wiesbaden*) **124,** 109 (1981).
6. A. G. Andersen, T. Hayakawa, K. Suzuki, M. Shimizu, and K. Takehira, *Catal. Lett*. **27,** 221 (1994).
7. M. Misono and T. Nitadori, *Stud. Surf. Sci. Catal.* **21,** 409 (1985).
8. T. Shimizu, *Appl. Catal.* **28,** 81 (1986).
9. J. J. Liang and H. S. Weng, *Ind. Eng. Chem. Res.* **32,** 2563 (1993).
10. H. Taguchi and Y. Takahashi, *J. Mater. Sci. Lett*. **3,** 251 (1984).
11. T. Hayakawa, A. G. Andersen, H. Orita, M. Shimizu, and K. Takehira, *Catal. Lett*. **16**, 373 (1992).
12. A. G. Andersen, T. Hayakawa, T. Tsunoda, H. Orita, M. Shimizu, and K. Takehira, *Catal. Lett*. **18,** 37 (1993).
13. Y. Matsumoto, J. Kurimoto, and E. Sato, *J. Electroanal. Chem.* **102,** 77 (1979).
14. Y. Matsumoto, J. Kurimoto, and E. Sato, *Electrochim. Acta* **25,** 539 (1980).
15. Y. Takeda, R. Kanno, T. Kondo, O. Yamamoto, H. Taguchi, M. Shimada, and M. Koizumi, *J. Appl. Electrochem.* **12,** 275 (1982).
16. J. C. Grenier, N. Ea, and M. Pouchard, *Rev. Chim. Miner.* **21,** 692 (1984).
17. G. O. Lauvstad, R. Tunold, and S. Sunde, *Proc. Electrochem. Soc.* **95**(1), 731 (1995).
18. T. Norby, P. H. Middleton, E. W. Hansen, I. Dahl, and A. G. Andersen, *Chem. Eng. Technol.* **18,** 139 (1995).
19. N. E. Trofimenko, H. Ullmann, J. Paulsen, and R. Muller, *Solid State Ionics* **99,** 201 (1997).
20. S. Shin, Y. Hatakeyama, K. Ogawa, and K. Shimomura, *Mater. Res. Bull.* **14,** 133 (1979).
21. Y. Takeda, K. Kanno, T. Takada, O. Yamamoto, M. Takano, N. Nakayama, and Y. Bando, *J. Solid State Chem.* **63,** 237 (1986).
22. P. K. Gallagher, J. B. MacChesney, and D. N. E. Buchanan, *J. Chem. Phys.* **41,** 2429, (1964).
23. B. C. Tofield, C. Greaves, and B. E. F. Fender, *Mater. Res. Bull.* **10,** 737 (1975).
24. M. Takano and Y. Takeda, *Bull. Inst. Chem. Res., Kyoto Univ.* **61,** 406 (1983).
25. A. A. Colville, *Acta Crystallogr., Sect B* **26,** 1469 (1970).
26. J. Berggren, *Acta Chem. Scand.* **25,** 3616 (1971).
27. T. C. Gibb, A. J. Herod, D. C. Munro, and N. Peng, *J. Mater. Chem.* **5,** 1909 (1995).
28. T. C. Gibb, A. J. Herod, D. C. Munro, and N. Peng, *J. Mater. Chem.* **4,** 1451 (1994).
29. J. B. MacChesney, R. C. Sherwood, and J. F. Potter, *J. Chem. Phys.* **43,** 1907 (1965).
30. Y. Takeda, S. Naka, M. Takano, T. Shinjo, T. Takada, and M. Shimada, *Mater. Res. Bull.* **13,** 61 (1978).
31. A. G. Alvarez, P. J. Aymonino, E. J. Baran, L. A. Gentil, A. H. Lanfranconi, and E. L. Varetti, *J. Inorg. Nucl. Chem.* **38,** 221 (1976).
32. R. A. Young, A. Sakthivel, T. S. Moss, and C. O. Paiva-Santos, *J. Appl. Crystallogr.* **28,** 366 (1995).
33. C. H. Giles and A. S. Trivedi, *Chem. Ind.* (*London*) 1426 (1969).
34. C. O. Della Vedova, J. H. Lesk, E. L. Varetti, P. J. Aymonino, O. E. Piro, B. E. Rivero, and E. E. Castellano, *J. Mol. Struct*. **70,** 241 (1981).
35. Powder Diffraction File No. 25-1402.
36. P. E. Werner, *Ark. Kemi* **31,** 513 (1969).
37. S. D. Ross, "Inorganic Infrared and Raman Spectra." McGraw-Hill, London, 1972.
38. I. J. Moraes, M. C. Terrile, O. R. Nascimento, M. Siu Li, R. H. Porto Francisco, and J. R. Lechat, *Mater. Res. Bull.* **27,** 523 (1992).
39. T. Nishida, S. Kubuki, M. Shibata, Y. Maeda, and T. Tamaki, *J. Mater. Chem.* **7,** 1801 (1997).
40. P. Ganguly and N. Y. Vasanthacharya, *J. Solid State Chem.* **61,** 164 (1986).
41. S. L. Cuffini, V. A. Macagno, R. E. Carbonio, A. Melo, E. Trollund, and J. L. Gautier, *J. Solid State Chem.* **105,** 161 (1993).
42. J. B. MacChesney, P. K. Gallagher, and D. N. E. Buchanan, *J. Chem. Phys.* **43,** 1907 (1965).
43. S. Nakamura and S. Iida, *Jpn. J. Appl. Phys., Part. 2* **34,** L291 (1995).